Investigation on the properties of high-pressure torsion (HPT) processed Al/B$_4$C composite

Sina Hadi, Mohammad Hossein Paydar*

Department of Materials Science and Engineering, School of Engineering, Shiraz University, Shiraz, Iran.

ABSTRACT

In the present work, commercially pure Al powder and Al-B$_4$C powder mixture including 5 to 20 wt. % B$_4$C particles, were consolidated to disc shape samples through applying high pressure torsion process at room temperature. To study the microstructural characteristics and evaluating the mechanical properties of the fabricated samples SEM, microhardness and shear punch test experiments were performed, respectively. It has been found that, by applying high compression pressure and even without applying torsion, full density can be reached in consolidation of the composites including lower than 5 wt% of B$_4$C particles. For the samples include more reinforcement, applying torsional strain (1 to 3 turns), plus high compression pressure although has a significant effect on redistribution of B$_4$C particles in the Al matrix, but could not lead to full density. The results also showed that microhardness values increase by increasing B$_4$C content, only if enough torsional strain were applied. The same trend was also recorded for the maximum shear strength, so that it is justified not only by the amount of used reinforcement but also by the degree of consolidation.

Keywords: High Pressure Torsion, Aluminum powder, B$_4$C, Consolidation, Composite

1. Introduction

Severe plastic deformation (SPD) methods are renowned by many researchers for the production of bulk nanostructured and materials with sub-micrometer microstructure with superior mechanical properties. This method of deformation can be applied to bulk or even sheet and powder materials and showed advantages that can alter the grain size of the samples without any changes in their chemical composition or unfavorable deformities in their overall shape [1]. Among the various SPD processes, equal channels angular pressing (ECAP) [2, 3], high pressure torsion (HPT) [4, 5], accumulative roll bonding (ARB) [6, 7], constrained groove pressing (CGP) [8], twist extrusion (TE) [9], and simple shear extrusion (SSE) [10] are well known for producing ultra-fine grain materials. Early experiments on applying simultaneous compression and torsion to materials, which is known as HPT process can be traced in the works of Bridgman, [11] HPT is perhaps the most effective technique among other SPD techniques, which could be applied to the work piece more easily than other SPD techniques like ECAP and ARB [4].

Vast applications of HPT consist of efficiently producing ultra-fine grain sizes in the range of 1 (μm) to around 100 (nm) or even smaller in aluminum solid solutions [12] (however the minimum attainable grain size depends on the

processed material's SFE [13]), mechanical alloying of high entropy alloys [14], fabricating composites [15] and to promote the consolidation of the metallic [16] and ceramic powders [17]. Based on the restriction on the path of the material flow, the HPT process is divided into 3 types, namely; unconstrained, constrained and semi-constrained. The semi-constrained form is the most common and effective type of the HPT process. In this type of HPT process each die contains a hollow round cavity, which has a shallow depth [18]. These cavities prevent the excessive lateral flow of the material. SPD methods also HPT due to high shearing strain imposed to the material [19] usually lead to crushing of the native alumina or aluminum hydroxide layer on the surface of aluminum powder particles that cause creation of fresh metallic surface to be cold welded during applied pressure. Furthermore; the fine secondary phase dispersoids removed from surface of the Al particles, are distributed in the consolidated aluminum matrix and results in excellent strength and thermal stability of the ultra-fine grained (UFG) microstructure created after subjecting the material to SPD process [20]. If the initial powder includes finer particles, this effect becomes more remarkable since in this case the fraction of native surface phases would be relatively large [21]. Numerous investigations focused on HPT-processing of different types of PM composites based on Cu, Ti, Mg [22-24], pure aluminum powder and aluminum matrix composites [21, 25, 26]. These research works proved that high strength, good ductility as well as high microhardness values could be obtained for pure aluminum powders consolidated at room temperature by the HPT process.

Khajouei-Nezhad et al [25], investigated the microstructural and mechanical properties of the pure Al powder which was consolidated by unconstrained HPT process. The relative density measurements for the samples, which processed for 1, 2 and 4 turns of HPT and under the pressure of 1.2 (GPa), exhibits that after 4 turns of torsion the samples didn't reach the full density. Bachmaier and Pippan [21] studied the effect of powder particle size on the microstructure and microhardness of the HPT processed samples. They used two types of Al powders with various particle sizes. Based on their results, it can be concluded that in the case of powder consolidation by applying SPD process, the finer initial particle size would result in smaller grain sizes and even obtaining ultra fine grained structure.

Zhang et al. [27] fabricated the Al-B_4C composite with various volume contents of B_4C (5, 10, 15, 20 and 25) by vacuum hot pressing sintering at 680^{0}C. They reported that the maximum relative density of 99.2 percent was attained for Al-5 vol% B_4C composite and the maximum hardness of about 108 Vickers was obtained for the composite including 25 vol% of B_4C. Paidar et al. investigated the effect of multi friction stir processing (FSP) passes on the microstructure, mechanical, wear and fracture behaviors of the fabricated 10 cycle ARB processed Al-2%B_4C composites. The fragmentation and distribution level which represents the homogeneity of B_4C particles in the Al matrix improve with the increase in the number of FSP passes [28]. Garechomaghlu and Mirzadeh investigated the effect of ARB on the mechanical properties and ductility of a typical particulate Al-B_4C composite. They showed that by increasing the ARB pass number, the tensile strength and total elongation of composites increase. It was also determined that the effect of particle distribution on the ductility is more sensible than the tensile strength [29].

In the present study, semi-constrained HPT process was applied for consolidation of pure Al powder and Al/B_4C composite powder including different weight percent of B_4C, at room temperature. Processed disks were subjected to density measurements, microhardness and shear punch test evaluations to study the mechanical characteristics of the consolidated samples. Microstructural changes were also investigated by SEM.

2. Materials and Methods

The primary materials used in this study were commercially pure aluminum (99.99%) and B_4C powders with average particle sizes of 40 and 0.7 μm, respectively. For preparing the composite powder, Al powder was mixed with B_4C particles by using a jar mill in ethyl alcohol for 24 hours to achieve Al/B_4C mixture including 5, 10 and 20 weight percent of B_4C. Initial Al and Al/ B_4C disk samples were fabricated by compacting mixed powders by hydraulic press facility and die-punch tool with the diameter of 15 (mm) under the pressure of 200 (MPa). Precompacted disks were weighed and by measuring the thickness of the disks, their densities were calculated. Afterwards precompacted disks were processed by HPT press facility under the hydrostatic pressure of 3.8 (GPa) for 0, 1 and 3 turns of rotation with a speed of 0.25 RPM. The densities of HPT processed samples were

measured by Archimedes method. For studying the microhardness changes, Vickers microhardness measurements were carried out under the load of 200 g with dwell time of 15 seconds and the rate of 0.2 g.s^{-1} along the cross section of the samples. Among different methods of evaluating the mechanical properties of small samples, shear punch testing (SPT) due to several advantages like simplicity of the die and punch setup, the low amount of required material, and above all, the correlation of the achieved results with those of the common uniaxial tensile testing (UTT) method, attracted much attention. Fig.1 shows a schematic representation of the shear punch testing setup [30]. To carry out this test a shear punch fixture with a 3.21 mm diameter flat cylindrical punch and cross head speed of 0.2 mm/min was used. HPTed disks were grind and thinned to 0.7 mm of thickness and after locating the disks in the fixture, the applied load of
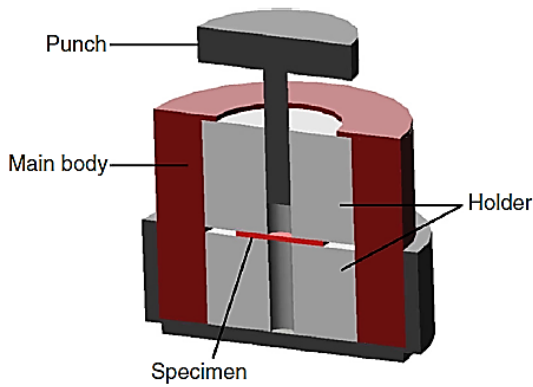
P was measured automatically as a function of the punch displacement and the data were recorded by a computer. By using the following relationship (eq. 1), the shear stress of the samples were estimated.

$$\tau = P/\pi dt \qquad (1)$$

Where τ is shear stress, t is the sample thickness and d is the average of the die and punch diameters.

Furthermore, for studying the microstructure of the specimens, polished cross sections of the disks were studied by SEM.

3. Results and discussion
3.1. Density evaluation

To study the properties of the HPT fabricated Al/B$_4$C composite, density measurements were performed on the samples before and after the process and obtained values were compared with the theoretical density values, which was calculated by applying the mixture rule and for each sample and processing situation is presented in Fig. 2. As it can be seen, for the precompacted samples, density is far from the full density. It means that by applying 200 MPa pressure in a single action uniaxial pressing process it is not possible to reach theoretical density, even for the pure Al powder. However, as it can be noted, by increasing the amount of B$_4$C in the composite samples, difference between the measured density and the theoretical density increases, which is completely comprehensible. The relative density of the HPT processed samples after zero (simple compression under applying 3.8 GPa pressure in semi-constrained HPT mode), 1 and 3

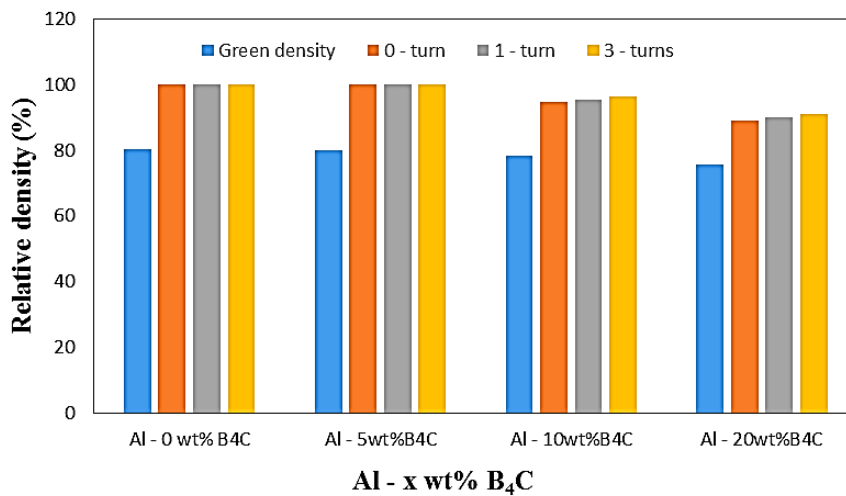Fig. 1- Schematic representation of the SPT die setup [30].

Fig. 2- Relative density before HPT and relative density of processed samples for 0, 1 and 3 turns of revolution.

turns of revolution is reported in Fig. 2. According to this figure, for pure Al and Al-5wt%B_4C composite the full density was achieved for all applied HPT processing conditions. This surely originates from two factors; first the lack of undeformable B_4C particles in the soft pure Al matrix and low amount of these particles in Al-5wt%B_4C and second the semi-constraint condition of the dies in which due to the restrictions against the flow of the material, higher amounts of the hydrostatic pressure and subsequently heavier deformation acts on the sample. By increasing the B_4C content to 10 and 20 weight percent, relative density values decrease. Although by applying torsional deformation for 1 and 3 turns relative density showed increase but again achieving full density was out of access. This problem refers to the amount of B_4C particles. The more increase in B_4C weight percent, due to ceramics intrinsic characteristics, results in lower final density.

3.2. Microstructure

The microstructural changes during HPT process was investigated by SEM analysis. Fig. 3 shows the pure Al microstructure fabricated by HPT process under applying zero (simple compression), 1 and

3 turns of revolution. Considering Fig. 3a, 3b and 3c, in which a uniform microstructure without any voids and porosities were obtained, implies the prosperity of the semi constraint HPT process in complete consolidation of pure Al samples.

In Fig. 4, the microstructure of the Al-5wt%B_4C is shown. For the sample fabricated by simple compression in HPT process (Fig. 4a), the clusters of B_4C can be seen in matrix as coarse and aggregated gray particles (see dotted yellow enclosures). By applying revolution for 1 and 3 turns (Fig. 4b and 4c), due to torsional strain imposed to the samples, these particles were rearranged and distributed more homogenously. Also, as it can be seen in SEM images for the Al-5wt%B_4C sample (Fig. 4a, b, c) there are no signs of porosity or cracking inside the microstructure which is in complete accordance with the measured density for this composite. Microstructure of the Al-10 wt%B_4C composite samples fabricated by HPT process is presented in Fig. 5. As it can be seen, the aggregated B_4C particles was coarser in the sample that fabricated under simple compression condition (Fig. 5a dotted yellow enclosures) and also porosities were visible (see black dotted enclosures) in the microstructure. By increasing the number of revolutions to 1 and
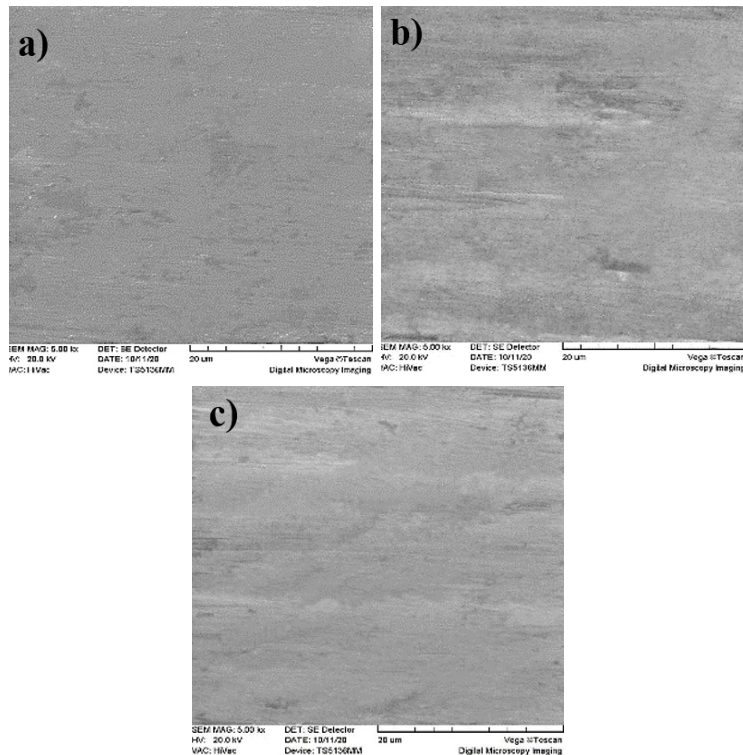

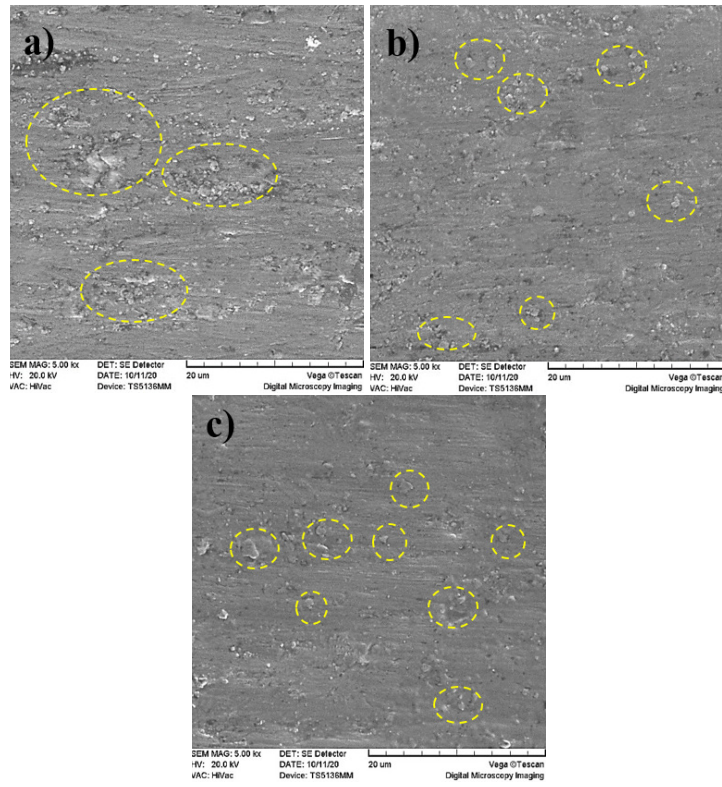Fig. 3- Pure Al a) simple compression, b) 1 turn, c) 3 turns.

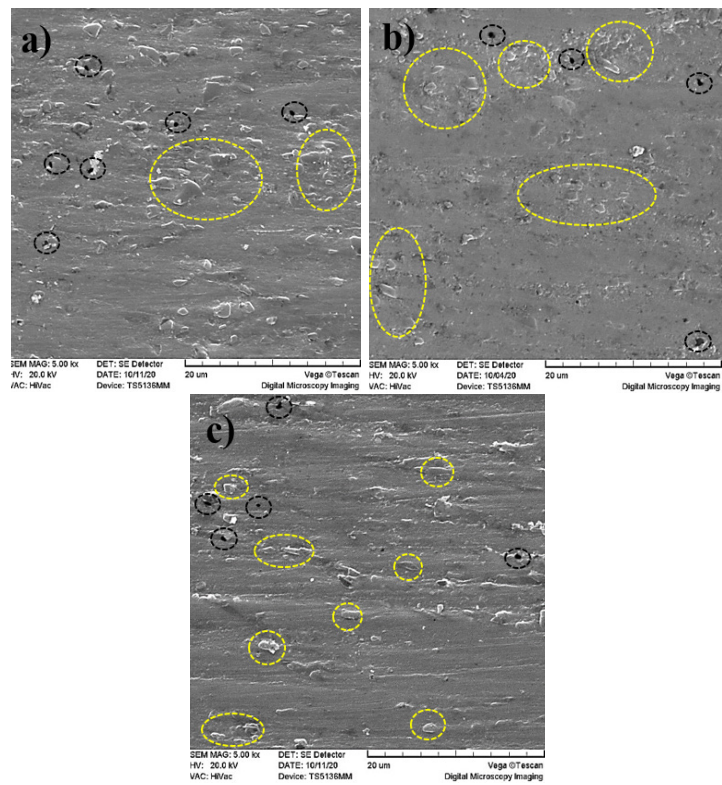Fig. 4- Al-5wt%B$_4$C a) simple compression, b) 1 turn, c) 3 turns.

Fig. 5- Al-10wt%B$_4$C a) simple compression, b) 1 turn, c) 3 turns.

3 turns, the clusters were crushed and particles were redistributed and more homogenous and finer microstructure were achieved (Fig. 4b, 4c). By regarding the black dotted enclosed regions, it can be noted that the porosities were not completed eliminated. For the Al-20wt%B_4C composite, Fig. 6 represents the microstructure of the samples. In Fig. 6a, B_4C particles are appeared as very coarse and elongated layers (yellow dotted enclosures) for simple compression condition, which some of the particles were detached from these layers during the grinding process. Also, in a wide zone (the black dotted enclosed region) a complex of big pores and cracks can be seen clearly. In this case it can also be recognized that after applying torsional deformation to the samples for 1 and 3 turns, the pores became finer and distribution of the B_4C particles was modified and were dispersed at farther distances from each other, although some porosities yet were existed in the microstructure and could not be eliminated (Fig. 6b, 6c).

This fact that the best densification behavior and highest density values was achieved for the samples include the lowest amount of B_4C, and that by increasing the content of B_4C reinforcement particles porosities and cracks could not be eliminated completely, even by applying torsional strain, refers to this phenomena that the densification in composite materials including hard reinforcement such as Al_2O_3, B_4C, BN, SiC, TiC, TiN etc. is limited due to the presence of the hard undeformable ceramic particles. In fact, hard ceramic particles prevent free flow of soft Al matrix, which means that the formability of the aluminum matrix, which plays a determinative roll in improving density under applied pressure and torsional strain, would be remarkably diminished by the presence of hard ceramic reinforcement. It was found by researchers that the enhanced densification could be achieved by closure of the pores within the microstructure, that can be reached by diffusion during sintering process or plastic flow as a result of applied stress. For the metallic composites by increasing the content of the ceramic hard particles in metal matrix, removal of the pores would be impeded due to decreasing deformability of the composite, so the efficient densification cannot be reached [28, 31, 32].
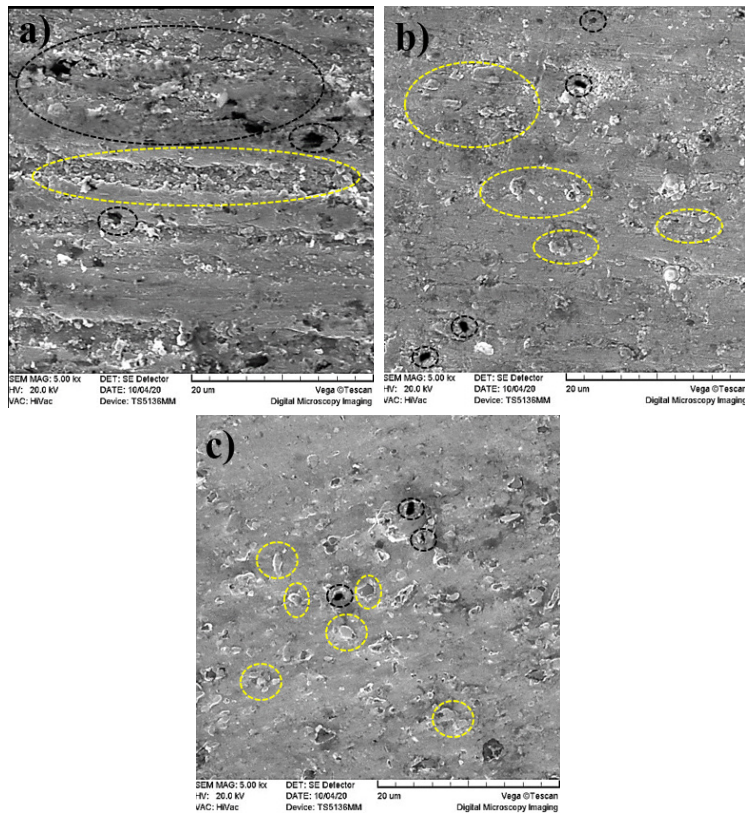

Fig. 6- Al-20wt%B_4C a) simple compression, b) 1 turn, c) 3 turns.

Regarding this fact, the higher contents of B_4C, as measured density values was also proved, resulted in lower densities and larger remained porosities and cracks within the microstructure. Therefore, in higher contents of B_4C in which the particles distribution wasn't fragmented efficiently, these pores and cracks could predispose the material to failure. By the way, by applying more torsional strain to the samples, due to the fragmentation and better dispersion of the hard boron carbide particles in the aluminum matrix, the mechanical properties was improved.

3.3. Microhardness of HPT deformed disks

Microhardness evaluations along the radius on the shear plane of the HPT deformed samples, showed considerable effect of oxide and reinforcement particles on microhardness. As it can be seen in Fig. 7, for the consolidated Al powder specimens by increasing the number of turns higher amounts of microhardness achieved. Regarding this fact that in HPT process by approaching from center to edges the applied strain increases, microhardness values is expected to show higher values for peripheral in comparison with the central zones. By increasing the number of revolutions, due to higher amounts of strain induced to the material, microhardness values showed a considerable ascending trend.

Fig. 8, shows the microhardness changes for Al-$5wt\%B_4C$ composite from the center point toward the edges. As it can be seen, the ascending behavior of the microhardness values by increasing the number of revolutions was preserved. Besides due to the reinforcement role of B_4C particles in Al matrix, higher values for microhardness was achieved. By applying torsional deformation, induced heavy
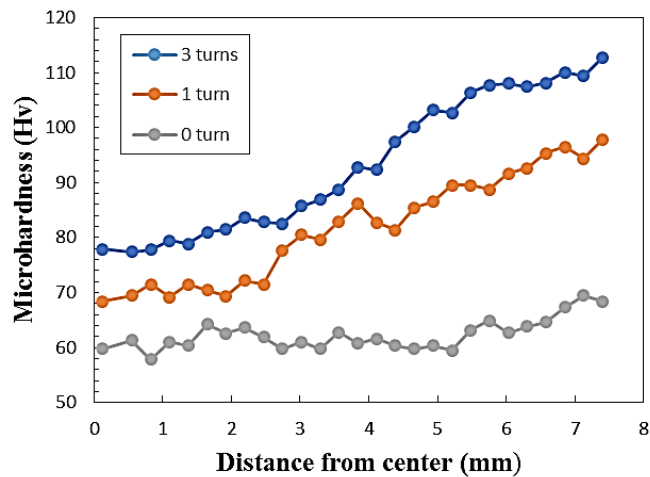

Fig. 7- Microhardness evolution for pure Al samples for simple compression, 1 turn and 3 turns of revolution.
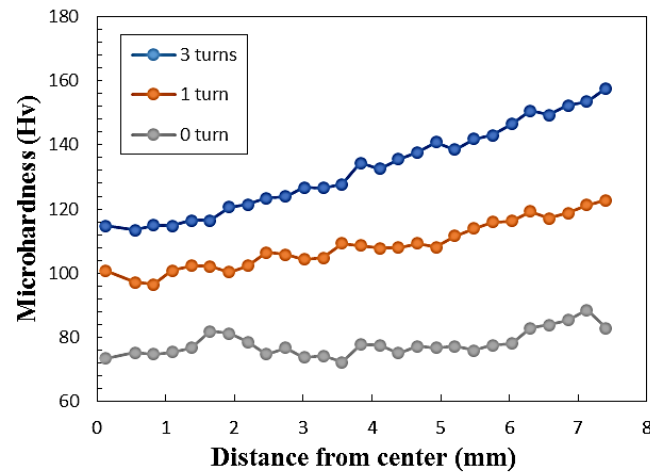

Fig. 8- Microhardness evolutions for Al with 5wt% of B_4C composite samples for simple compression, 1 and 3 turns of revolution.

shear strain, not only the B_4C particles distributed more homogenously but also more perfect bonding between aluminum particles could be expected, that both can results in higher micro hardness. Furthermore, it also causes the native Al_2O_3 layer on the powder particles to break and spreading these crushed oxide particles in the aluminum matrix leads to higher microhardness values and homogenous microstructure. By increasing the content of B_4C, because of the reinforcing nature of the B_4C particles the microhardness values would increase too. The microhardness values for the fabricated composites including 10 and 20 weight percent of B_4C are presented in Fig. 9 and 10, respectively. As mentioned before achieving higher values of micro hardness is logically expected when the reinforcement particle's percentage increase. For the Al-10 wt%B_4C composite (Fig. 9)

the effect of B_4C addition on the micro hardness of the fabricated composite is the same as what is expected and an increase in micro hardness with respect to the sample including 5 wt% B_4C can be recognized. Although the increase in micro hardness is not enough high that can be because of lower relative densities for the samples included 10 wt% of B_4C. For the samples include 20 wt% B_4C, the effect of density on the microhardness is more pronounced. In the other words, for these samples although the amount of B_4C reinforcement is high and it is expected to have a huge influence on the microhardness, but at the same time they decrease formability of the composite and prevent perfect consolidation that caused a negative effect on micro hardness. By the way, as it can be seen clearly in Fig. 10, by increasing the turn number of revolutions in HPT process, higher microhardness achieved
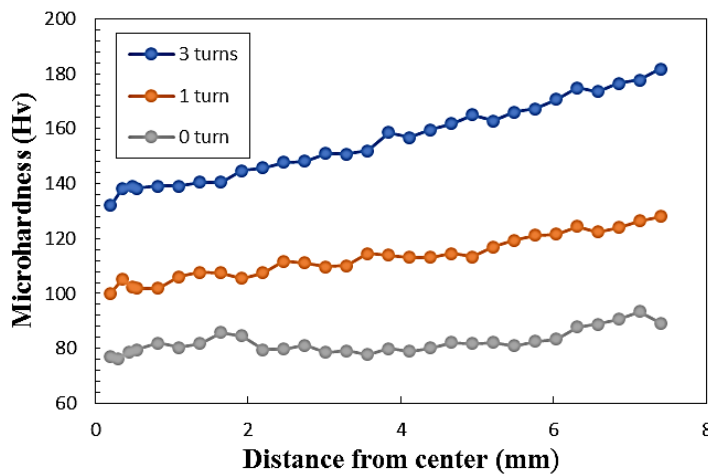

Fig. 9- Microhardness evolutions for Al with 10wt% of B_4C composite samples for simple compression, 1 and 3 turns of revolution.
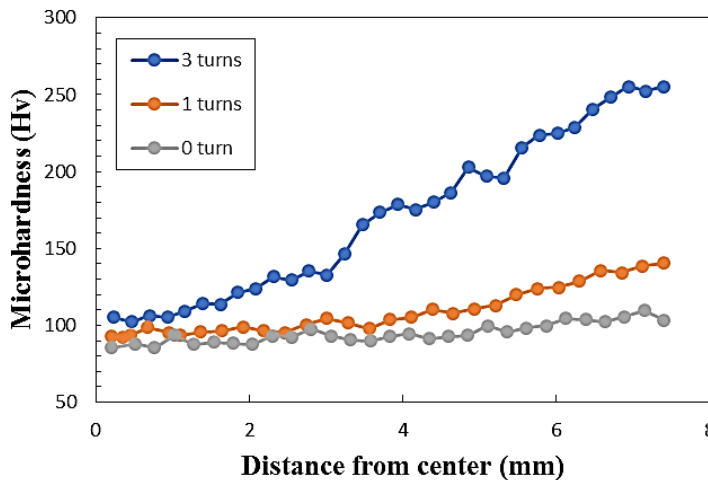

Fig. 10- Microhardness evolutions for Al with 20 wt% of B_4C composite samples for simple compression, 1 and 3 turns of revolution.

especially in far from center of the disk samples due to higher applied shear strain and better consolidation and redistribution of B_4C particles. In current study, full density was achieved by simple compression in HPT process for pure Al and Al-5wt% B_4C and microhardness values reached above 110 and 150 Vickers for these samples after 3 turns of revolution. Comparing the results obtained by current research with aforementioned cases such as what studied by Zheng et al [26], in which Al-B_4C composites including different amount of B_4C were fabricated by vacuum hot press sintering process, it can be seen that they couldn't obtain full density and microhardness values didn't approach the values more than 108 Vickers. Also, in the case of HPT processed composites, Khajouei-Nezhad et al [24] showed that even after 4 turns of revolution, the full density wasn't obtained, which directly corresponds to the unconstrained dies used in that study. The effect of powder particle size on the mechanical properties was also discussed by Bachmaier and Pippan [20]. They found that smaller particles would result in finer grain sizes in UFG range. By considering this fact and powder particle sizes which used in the current work it can be concluded that the UFG structure could have achieved.

3.4. Shear punch testing of the processed disks

For evaluating the mechanical behavior of the pure Al and composite consolidated disks, shear punch test (SPT) was performed for the zero (simple compression) and 3 turns HPT processed samples. Fig.11 shows the shear strength against normalized displacement for the pure Al samples. As it can be

seen, no big difference between the results obtained for these two samples can be noted, that is probably due to the full density achieved for pure Al powder in applying 0 and 3 turns HPT process (Fig. 3). By the way, by applying 3 turns of revolution to the pure Al sample, heavy amounts of strain induced to the material that caused considerable work hardening, which in turn, leaded to an increase in the shear strength of the consolidated sample.

In Fig. 12 shear strength against normalized displacement for the Al-5wt%B_4C is demonstrated. It can be seen that for 3 turns of revolution due to higher amounts of strain applied to the material and also redistribution of B_4C particles, a remarkable increase was happened in shear strength. For the Al-10 wt%B_4C sample (Fig. 13) unexpectedly lower shear strength than the sample includes 5 wt% B_4C was recorded. This could be interpreted with regarding the relative density of the processed Al-10wt%B_4C samples presented in Fig. 2. Relative density values for simple compression and 3 turns were not reached the full density, which indicates that the samples have some amount of remained porosities. The remained porosities cause the failure of the material during the shear punch test and lower shear strength. In Fig. 14 the SPT curves for Al-20wt%B_4C samples are illustrated. As it can be seen there is no significant increase or improvement in shear strength of the samples comparing with the shear strength obtained for the pure sample and much lower than what obtained for the composite samples including 5 or even 10 wt% of B_4C. This is due to the lower relative density and higher remained porosities for the samples include high amount of B_4C, even for consolidated by
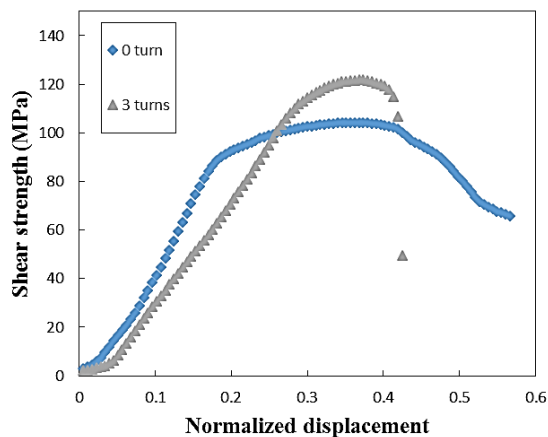

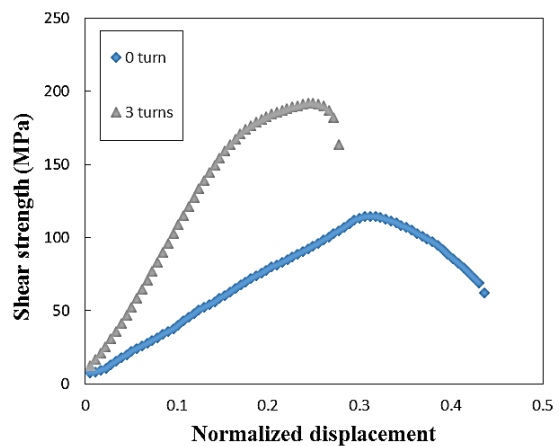Fig. 11- SPT curve for pure Al samples subjected to simple compression and 3 turns of revolution.

Fig. 12- SPT curve for Al-5%wtB_4C samples subjected to simple compression and 3 turns of revolution.

applying 3 turns HPT process. In the other words, high amount of reinforcement could be useful in improving strength of the fabricated composite, just if the density of the consolidated composite reach to full density and also the reinforcement particles are distributed homogenously and are not present in the form of clusters.

Yield strength of the SPT samples can also be calculated by multiplying the maximum shear strength of material (which obtained from shear punch test) to $\sqrt{3}$. Fig. 15 shows the yield strength of the SPT samples. For all samples which subjected to 3 turns of revolution, yield strength is higher than those which endured zero turn. But this increase is remarkably higher for Al-5wt% B_4C sample. This could be explained by considering the density values for this composite. As clearly shown in Fig.2, Al-5wt% B_4C composite reached to full density condition even without applying

torsional deformation. This means that there are no porosities in this composite. Therefore, by applying 3 turns of revolution due to heavy strain induced to the material and high work hardening alongside no porosity, the yield strength shows considerable increase.

4. Conclusion

In the present work fabrication of Al-B_4C composites including 0 to 20 wt% B_4C via consolidation through HPT process has been studied. The results showed that by increasing the B_4C content the relative density decreases. For pure Al and Al-5wt%B_4C composite by applying just high enough pressure and without torsional deformation, full density could be achieved but by increasing the B_4C content to 10 and 20 weight percent the material couldn't reach the full relative density values even by applying torsional
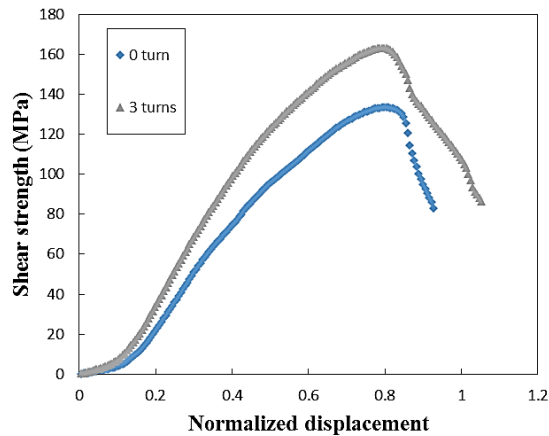

Fig. 13- SPT curve for Al-10%wtB_4C samples subjected to simple compression and 3 turns of revolution.
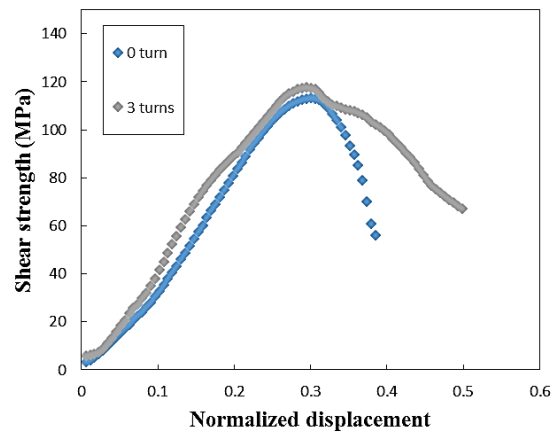

Fig. 14- SPT curve for Al-20%wtB_4C samples subjected to simple compression and 3 turns of revolution.
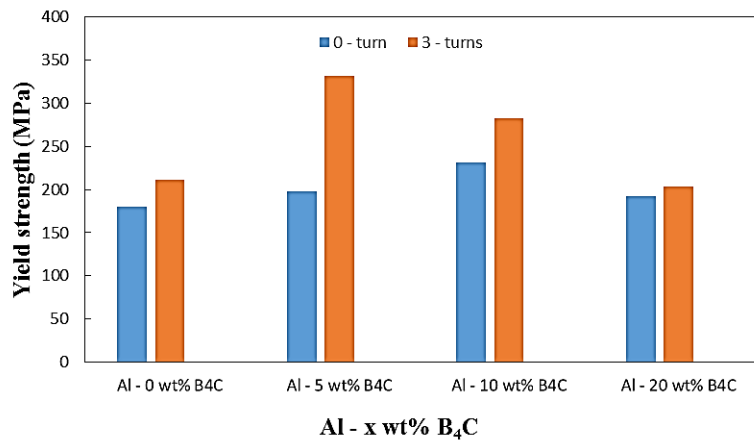

Fig. 15- Yield strength of shear punch test for pure Al and composite samples.

deformation. SEM images proved that by applying torsional deformation, reinforcement particles could be redistributed and be finely distributed in the matrix. Microhardness evaluations showed considerable effect of the B_4C content and torsional deformation on the measured values. In fact, with increasing the weight percentage of B_4C and applying 3 turns of revolution due to higher imposed strains and better distribution of the particles in the aluminum matrix hardness values showed remarkable increases. Shear punch test evaluations also carried out and the increase of the shear strength by using 5 wt% B_4C reinforcement and applying torsional deformation was clearly shown. For the higher amount of reinforcement content, shear strength decreased due to their lower relative density, although the effect of torsional strain and particle distribution on the strength of these materials were pronounced.

References

1. Rezvani A, Ebrahimi R. Investigation on the Deformation Behavior and Strain Distribution of Commercially Pure Aluminum after Circular Simple Shear Extrusion. Journal of ultra high grained and nanostructured materials. 52(1); (2019): 32-42.
2. Valiev RZ, Langdon TG. Principles of equal-channel angular pressing as a processing tool for grain refinement. Progress in Materials Science. 2006;51(7):881-981.
3. Torabi M, Eivani AR, Jafarian H, Salehi MT. Re-strengthen¬ing in AA6063 Alloy During Equal Channel Angular Pressing. Journal of Ultrafine Grained and Nanostructured Materials. 50(2); (2017): 90-7.
4. Zhilyaev A, Langdon T. Using high-pressure torsion for metal processing: Fundamentals and applications. Progress in Materials Science. 2008;53(6):893-979.
5. Hadi S, Rahimzadeh lotfabad F, Paydar MH, Ebrahimi R. New Mathematical Stress Analysis in the Compressive Stage of the High-Pressure Torsion Process. Metals and Materials International. 2020.
6. Alizadeh M, Paydar MH. Fabrication of nanostructure Al/SiCP composite by accumulative roll-bonding (ARB) process. Journal of Alloys and Compounds. 2010;492(1-2):231-5.
7. Mohammad Nejad Fard N, Mirzadeh H, Mohammad R, Cabrera JM. Accumulative roll bonding of aluminum/stainless steel sheets. Journal of Ultra fine Grained and Nanostructured Materials. 50(1); (2017): 1-5.
8. Asgari M, Honarpisheh M, Mansouri H. Experimental and Numerical Investigation of Mechanical Properties in the Ultrasonic Assisted constraint groove pressing process of copper sheets. Journal of Ultrafine Grained and Nanostructured Materials. 53(1); (2020):48-59.
9. Beygelzimer Y, Varyukhin V, Synkov S, Orlov D. Useful properties of twist extrusion. Materials Science and Engineering: A. 2009;503(1-2):14-7.
10. Pardis N, Ebrahimi R. Deformation behavior in Simple Shear Extrusion (SSE) as a new severe plastic deformation technique. Materials Science and Engineering: A. 2009;527(1-2):355-60.
11. Bridgman PW. On Torsion Combined with Compression. Journal of Applied Physics. 1943;14(6):273-83.

12. Islamgaliev RK, Yunusova NF, Sabirov IN, Sergueeva AV, Valiev RZ. Deformation behavior of nanostructured aluminum alloy processed by severe plastic deformation. Materials Science and Engineering: A. 2001;319-321:877-81.
13. Zhao Y.H, Zhu Y.T, Liao X.Z, Horita Z, Langdon TG, Influence of stacking-fault energy on microstructural characteristics of ultrafine-grain copper and copper–zinc alloys. Materials Science and. Eng. A. 463; (2007): 22-26.
14. Kilmametov A, Kulagin R, Mazilkin A, Seils S, Boll T, Heilmaier M, et al. High-pressure torsion driven mechanical alloying of CoCrFeMnNi high entropy alloy. Scripta Materialia. 2019;158:29-33.
15. Xue Y, Jiang B, Bourgeois L, Dai P, Mitome M, Zhang C, et al. Aluminum matrix composites reinforced with multi-walled boron nitride nanotubes fabricated by a high-pressure torsion technique. Materials & Design. 2015;88:451-60.
16. Borchers C, Garve C, Tiegel M, Deutges M, Herz A, Edalati K, et al. Nanocrystalline steel obtained by mechanical alloying of iron and graphite subsequently compacted by high-pressure torsion. Acta Materialia. 2015;97:207-15.
17. Edalati K, Arimura M, Ikoma Y, Daio T, Miyata M, Smith DJ, et al. Plastic Deformation of BaTiO3Ceramics by High-pressure Torsion and Changes in Phase Transformations, Optical and Dielectric Properties. Materials Research Letters. 2015;3(4):216-21.
18. Figueiredo RB, Pereira PHR, Aguilar MTP, Cetlin PR, Langdon TG. Using finite element modeling to examine the temperature distribution in quasi-constrained high-pressure torsion. Acta Materialia. 2012;60(6-7):3190-8.
19. Paydar MH, Reihanian M, Bagherpour E, Sharifzadeh M, Zarinejad M, Dean TA. Equal channel angular pressing–forward extrusion (ECAP–FE) consolidation of Al particles. Materials & Design. 2009;30(3):429-32.
20. Balog M, Poletti C, Simancik F, Walcher M, Rajner W. The effect of native Al2O3 skin disruption on properties of fine Al powder compacts. Journal of Alloys and Compounds. 2011;509:S235-S8.
21. Bachmaier A, Pippan R. Effect of oxide particles on the stabilization and final microstructure in aluminium. Mater Sci Eng A Struct Mater. 2011;528(25-26):7589-95.
22. Akbarpour MR, Mousa Mirabad H, Alipour S, Kim HS. Enhanced tensile properties and electrical conductivity of Cu-CNT nanocomposites processed via the combination of flake powder metallurgy and high pressure torsion methods. Materials Science and Engineering: A. 2020;773:138888.
23. Li FX, Hao PD, Yi JH, Chen Z, Prashanth KG, Maity T, et al. Microstructure and strength of nano-/ultrafine-grained carbon nanotube-reinforced titanium composites processed by high-pressure torsion. Materials Science and Engineering: A. 2018;722:122-8.
24. Castro MM, Sabbaghianrad S, Pereira PHR, Mazzer EM, Isaac A, Langdon TG, et al. A magnesium-aluminium composite produced by high-pressure torsion. Journal of Alloys and Compounds. 2019;804:421-6.
25. Khajouei-Nezhad M, Paydar MH, Ebrahimi R, Jenei P, Nagy P, Gubicza J. Microstructure and mechanical properties of ultrafine-grained aluminum consolidated by high-pressure torsion. Materials Science and Engineering: A. 2017;682:501-8.
26. Ashida M, Horita Z, Kita T, Kato A. Production of Al/Al2O3 Nanocomposites through Consolidation by High-Pressure Torsion. MATERIALS TRANSACTIONS. 2012;53(1):13-6.
27. Zhang L, Wang Z, Li Q, Wu J, Shi G, Qi F, et al. Microtopography and mechanical properties of vacuum hot pressing Al/B4C composites. Ceramics International.

2018;44(3):3048-55.

28. Paidar M, Ojo OO, Ezatpour HR, Heidarzadeh A. Influence of multi-pass FSP on the microstructure, mechanical properties and tribological characterization of Al/B4C composite fabricated by accumulative roll bonding (ARB). Surface and Coatings Technology. 2019;361:159-69.

29. Gharechomaghlu M, Mirzadeh H. Toward understanding the origins of poor ductility in a metal-matrix composite processed by accumulative roll bonding (ARB). Archives of Civil and Mechanical Engineering. 2019;19(4):958-66.

30. Esfandyarpour MJ, Alizadeh R, Mahmudi R. Applicability of shear punch testing to the evaluation of hot tensile deformation parameters and constitutive analyses. Journal of Materials Research and Technology. 2019;8(1):996-1002.

31. Seetharam R, Subbu SK, Davidson MJ. Hot workability and densification behavior of sintered powder metallurgy Al-B 4 C preforms during upsetting. Journal of Manufacturing Processes. 2017;28:309-18.

32. Alihosseini H, Dehghani K, Kamali J. Microstructure characterization, mechanical properties, compressibility and sintering behavior of Al-B 4 C nanocomposite powders. Advanced Powder Technology. 2017;28(9):2126-34.